RRA-T703
1 March 1970

RRA RADIATION RESEARCH ASSOCIATES
Fort Worth, Texas

A COMPARISON OF CALCULATED AND MEASURED INTENSITIES OF SUNLIGHT REFLECTED BY THE EARTH'S ATMOSPHERE

C. Thompson and M B. Wells

Prepared under Contract NAS2-5285 for
THE AMES RESEARCH CENTER
NATIONAL AERONAUTICS AND SPACE ADMINISTRATION
Moffett Field, California 94035

A COMPARISON OF CALCULATED AND MEASURED INTENSITIES OF SUN LIGHT REFLECTED BY THE EARTH'S ATMOSPHERE

C Thompson and M. B. Wells

Prepared under Contract NAS2-5285
for the Ames Research Center
National Aeronautics and Space Administration
Moffett Field, California 94035

RADIATION RESEARCH ASSOCIATES, INC.
3550 Hulen Street
Fort Worth, Texas 76107

ABSTRACT

This report describes calculations that were performed to investigate the application of a computer procedure, RRA-89, developed under a previous contract to the computation of the irradiance received by a satellite. RRA-89 calculations of the total intensity of 0.37 and 0.78μ wavelength light at a satellite positioned over a clear maritime atmosphere were found to be in good agreement with calculations performed with the FLASH Monte Carlo procedure that treats a spherical shell atmosphere. LITE-II Monte Carlo calculations were run to determine the effect of changes in the type of surface albedo on the reflected radiation at the top of the atmosphere. LITE-II calculations were run to determine the effect of cloud optical thickness on the reflected radiation. Comparisons were made of the reflected intensities computed for a maritime atmosphere containing clouds with measured data from the Tiros satellite.

LITE-II calculations were run to determine the intensity of the atmospheric reflected sunlight from clear and cloudy maritime and clear continental atmospheres for wavelengths of 0.37, 0.45, 0.54, 0.67, and 0.78μ. These data were compared with OSO-III measurements for the same wavelength. The agreement found between the calculated and measured data is sufficiently close to warrant the conclusion that most problems involving the reflected radiation from the earth's atmosphere can be solved using the LITE-II data with the RRA-89 procedure.

LIST OF FIGURES

TABLE OF CONTENTS

Fig. Page

LIST OF TABLES

LIST OF TABLES (Cont'd)

I. INTRODUCTION

This report describes the work performed under NASA contract NAS-2-5285. The purpose of work described in this report was to evaluate the use of the LITE II (Ref. 1 and 2) Monte Carlo Code for the computation of the irradiance to a near earth spacecraft due to scattered and reflected sunlight, and to evaluate the range of angles between the spacecraft and subsolar point that the RRA-89 integration code (Ref. 3) could be used to determine the total intensity at the spacecraft.

The OSO-III earth albedo experiment data were used to determine the validity of the Monte Carlo calculations. The intensity per steradian of sunlight reflected from the earth's atmosphere as a function of wavelength, zenith angle of incidence, polar reflection angle and azimuthal reflection angle calculated by LITE-II was compared with measured data from the OSO-III spacecraft.

Model atmospheres were formulated to describe a clear maritime atmosphere, a clear continental atmosphere, and a maritime atmosphere with a thick stratocumulus cloud. Model maritime atmospheres with two somewhat optically thinner clouds were also formulated to investigate the angular distribution of the reflected sunlight observed above the atmosphere as a function of cloud thickness. The LITE-II Monte Carlo calculations for the model atmospheres were run for five wavelengths: 0.37μ, 0.45μ, 0.54μ, 0.67μ, and 0.78 μ. For

each model atmosphere ten incident solar angles were considered: 0°, 10°, 20°, 30°, 40°, 50°, 60°, 70°, 80°, and 85°. The angular distributions of the intensities in each model atmosphere were determined for ten surface albedos varying from 0.0 to 0.9 in steps of 0.1. The printed output of the LITE-II computations for a given solar zenith angle is displayed as a function of a polar reflection angle, and an azimuthal reflection angle relative to the sun position. These LITE-II calculations were made for two different receiver positions. One receiver was placed at the top of the atmosphere, thereby calculating the intensity of the radiation escaping from the top of the atmosphere. The calculations for the receiver position were both printed and stored on tape. These tapes may be used as input for the RRA-89 procedure. The second receiver was placed at 11 kilometers altitude; however, the scattered intensities for that receiver were printed only and not stored on magnetic tape.

Studies were made to determine the effect of the atmospheric optical thickness, ground albedo model, and single scattering albedo on the angular distribution of radiation reflected from the earth's atmosphere.

II. MODEL ATMOSPHERES

To calculate the intensity of the light observed by a receiver on a near earth spacecraft, a model of the atmosphere must be formulated. The atmospheric model is a function of the meteorological parameters, altitude and the wavelength of the observed light.

Because of the wide range of meteorological conditions encountered by the OSO-III spacecraft, a number of different atmospheric models were used. For the measurements over the ocean with a clear atmosphere, the Haze M model of Ref. 4 was used. For this model the distribution of particle sizes were taken to be given by the equation

$$n(r) = 5.333 \times 10^{-4}\, re^{-8.944 r^{1/2}} \qquad (1)$$

The particle density was taken to be 100 cm^{-3} and the Rayleigh scattering coefficient and ozone absorption coefficient as a function of altitude were interpolated from the data of Ref. 5. The atmosphere model was formulated in 1.0 km layers up to an altitude of 50 km. It was assumed that the ground level visibility (meteorological range) was 25 km.

The size distribution for the aerosols contained in the atmosphere over a continental land mass was represented by the Haze L model (Ref. 4). The size distribution function described in Equation 1 was used with the various constants being modified. The Haze L model represents a continental haze model with no clouds present. The Haze L size distribution is given by the equation

$$n(r) = 4.9757 \times 10^{6} r^{2} e^{-15.1186 r^{1/2}} \qquad (2)$$

The Haze L model atmosphere was also used in a study of the changes in the angular distribution of the reflected light with different ground albedos. Three problems were run with an isotropic scattering surface rather than a Lambert reflecting surface.

LITE-II problems were run for three different cloud models. The model specified as a stratus cloud was the stratus cloud model described in Ref. 6. The stratus cloud has an optical thickness of approximately 80. This model is so optically thick that the ground surface albedo has no effect on the light reflected from the top of the atmosphere. Two other cloud models were formulated using the size distribution described by Equation 1. The optical thicknesses were chosen to be 10 and approximately 0.1. In both cases it was possible to detect changes in the intensities as a result of changes in the ground surface albedo.

For all model atmospheres, microscopic aerosol scattering data, based on Mie theory, must be generated. In the Mie calculations, the index of refraction of the aerosol particles was taken to be 1.33. The aerosol phase functions data was generated by the use of RRA-42 (Ref. 2) for aerosol size parameters from 0.06 to 197. RRA-42 generated a BCD-library tape for the RRA-45 (Ref. 2) procedure which integrates the Mie data over the size distribution for the model in

question and produces macroscopic extinction and scattering coefficients, scattering phase functions and other pertinent probability functions that are necessary as input to the LITE-II procedure.

It was assumed in developing the model atmospheres that the atmospheres extend only to an altitude of 50 km. Ozone absorption was treated in the LITE-II calculations; however, for the wavelengths chosen for this study, the effect of water vapor and carbon dioxide absorption was neglected. In all of the model atmospheres the index of refraction of the aerosols was taken to be that of water and therefor the single scattering albedo for aerosols is unity.

III. LITE-II CALCULATIONS

The LITE-II Monte Carlo Code which was used to calculate the intensity per-steradian reflected from a plane parallel atmosphere is fully documented elsewhere (Ref. 2). Therefore, the calculational method will not be discussed here.

The intensity per steradian reflected from each of the model atmospheres described in the previous section was calculated for wavelengths of 0.37, 0.45, 0.54, 0.67, and 0.78μ as a function of the solar incidence angle, θ_o, the polar reflection angle, θ, and the azimuth angle of reflection, ϕ, relative to the sun. The geometry used for these calculations is shown in Fig. 1.

These intensities were calculated for two receiver positions, the first at 11 km altitude, and the second at 50 km, which was taken to be the top of the atmosphere. There were one hundred and fifteen LITE-II problems run for this study. The 11 km data was printed as a function of the polar view angle allowing the polar cosine to vary from +1.0 to -1.0 in 0.1 steps. For each polar view angle the intensities were calculated for six azimuth angle regions 30° wide. This data was printed only.

The data for the receiver positioned at the top of the atmosphere was printed and stored on tape for polar cosines from +1.0 to 0.0, and for six 30° wide azimuth regions. This data was also stored on magnetic tape for use as input to the RRA-89 procedure.

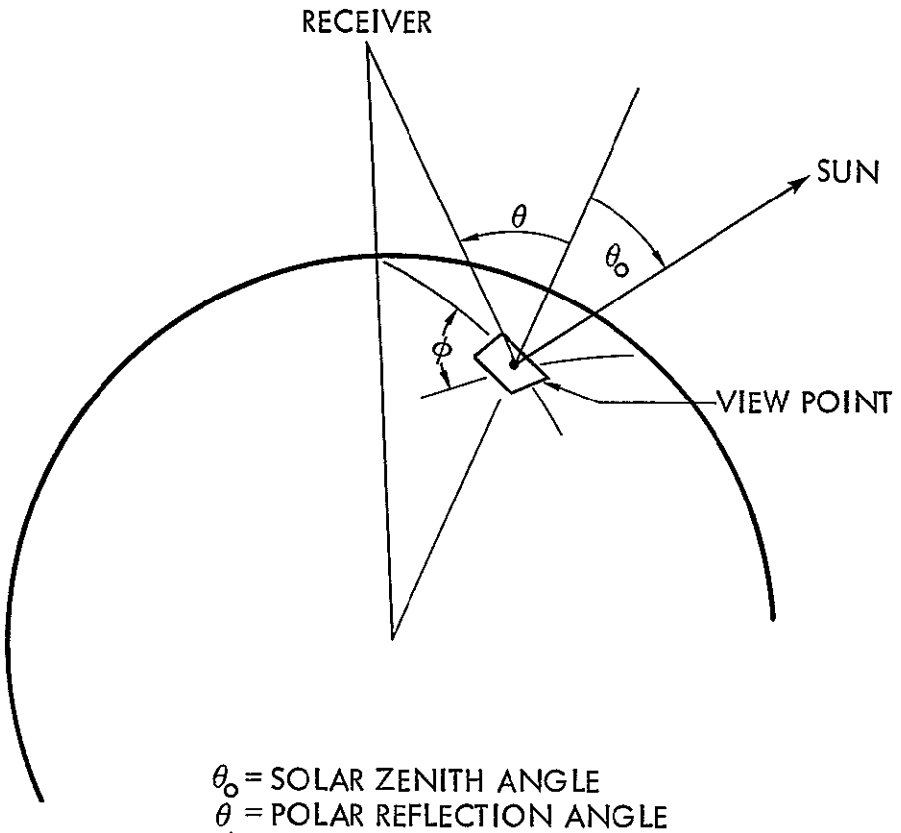

Fig. 1. View Point Geometry Used in Lite II

IV. COMPARISON OF INTENSITY CALCULATED BY RRA-89 WITH THOSE OF A SPHERICAL MODEL

The computer code designated as RRA-89 is an integration procedure that integrates the LITE-II calculated reflected intensity data over the top of the atmosphere that is illuminated by the sun to obtain the total reflected intensity at a satellite position for a spherical shell atmosphere. The reflected intensities calculated by the RRA-89 procedure for the Haze M atmosphere model and for wavelengths of 0.37μ and 0.78μ were compared with similar calculations from the FLASH Monte Carlo procedure (Ref. 7) which treats a spherical model atmosphere. Comparisons of the calculations from RRA-89 and FLASH giving the total intensity at a satellite positioned at an altitude of 300 nautical miles are shown in Fig. 2 and Fig. 3. These calculations are for ground surface albedos of 0.0 and 0.8. The total reflected intensity at the spacecraft is plotted as a function of the earth angle. The earth angle is the angle between the sub-satellite point and the sub-solar point measured at the center of the earth. It was felt that the RRA-89 code should not be used for large earth angles, due to the fact that the LITE-II data used as input to RRA-89 is for a plane parallel atmosphere.

The agreement between the RRA-89 and FLASH calculations is seen in Figs. 2 and 3 to be rather good. The largest disagreement between the two calculations is noted for $\lambda = 0.78\mu$ when the surface albedo

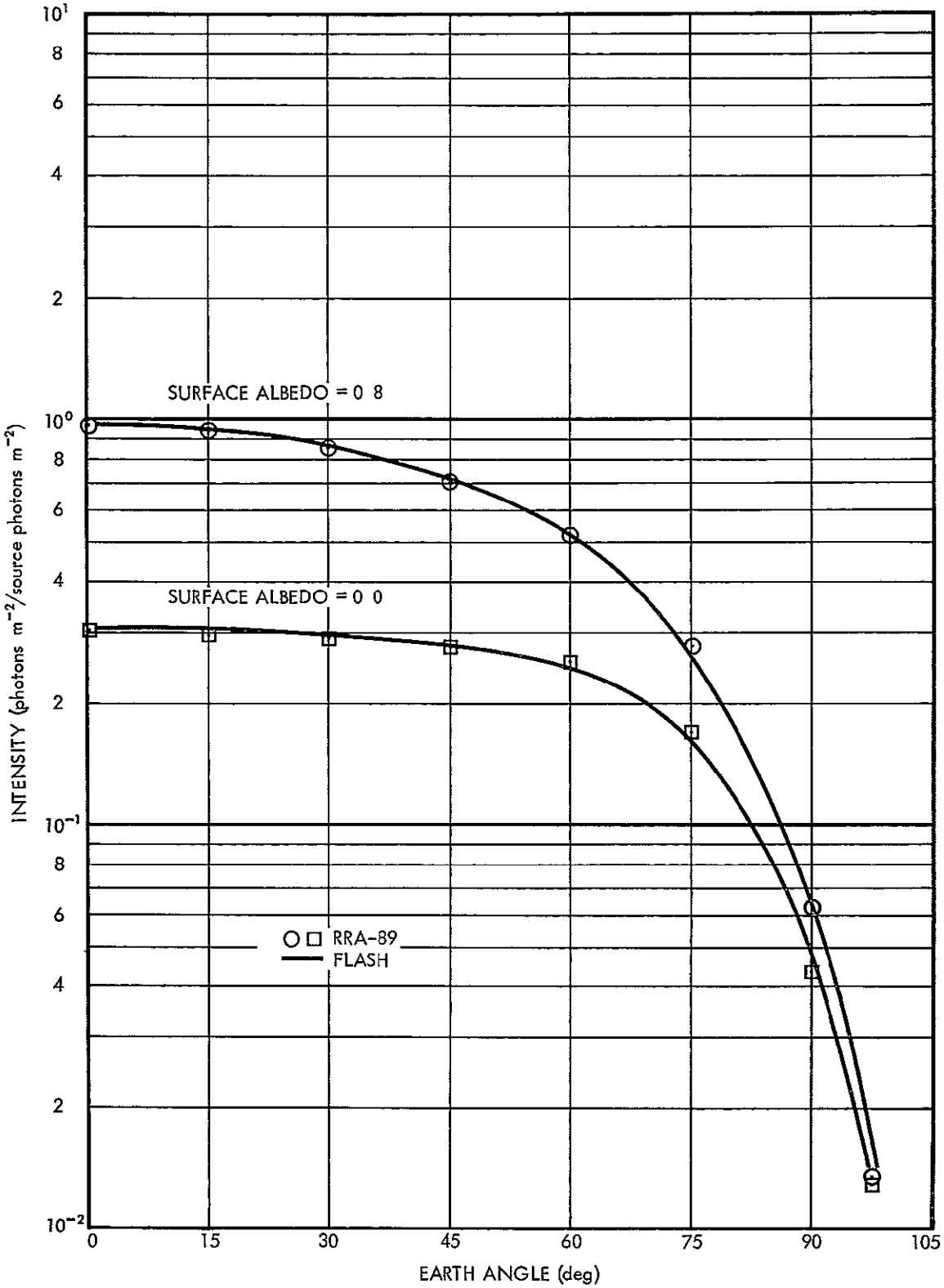

Fig. 2 Comparison of Data from a RRA-89 Calculation with Data from a Flash Calculation for a Wavelength of 0 37μ

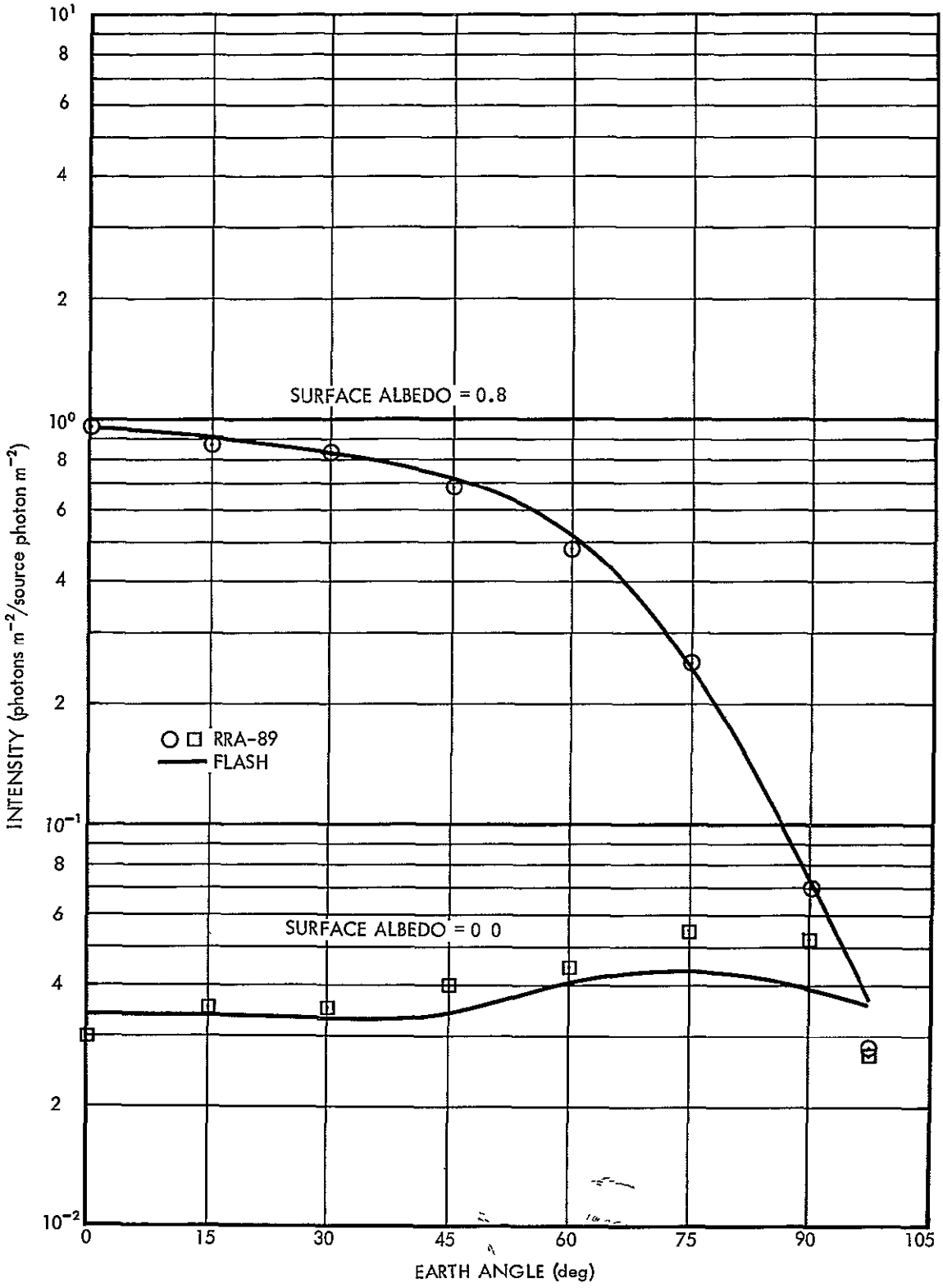

Fig 3 Comparison of Data from a RRA-89 Calculation with Data from a Flash Calculation for a Wavelength of 0 78μ

is 0.0. The mean-free-path thickness of the clear maritime atmosphere was taken to be 0.8450 for λ=0.37μ and 0.2145 for λ=0.78μ. The statistical accuracy of the FLASH calculations of the reflected intensities as well as those obtained from LITE-II, have been found to decrease with a decrease in the mean-free-path thickness of the atmosphere for a given number of histories used in the Monte Carlo calculations. Therefore, it is believed that the poorer agreement noted for the two calculations when the surface albedo = 0.0 and λ=0.78μ is due to the small sample size used in the FLASH calculation. The statistical variation in the FLASH results improve with an increase in the surface albedo. It is seen in both Figs. 2 and 3 that the FLASH and RRA-89 calculations for a surface albedo of 0.8 are in excellent agreement for earth angles to 90°. The FLASH calculations for a surface albedo of 0.8 indicates that RRA-89 might be possibly under estimating slightly the integrated intensity for earth angles greater than 90°.

From the comparisons shown in Figs. 2 and 3 it is concluded for wavelengths between 0.37μ and 0.78μ that the RRA-89 code will calculate the reflected intensity at a satellite position with reasonable accuracy for all earth angles less than 90°.

V. GROUND ALBEDO STUDIES

In the LITE-II calculations for the model atmospheres the ground has been considered as a Lambert surface. There was some question as to the effect of the type of ground surface on the angular distribution of the radiation emerging from the top of the atmosphere. A short study, assuming an isotropic surface albedo was conducted and compared to Monte Carlo calculations discussed in Section III which considered a Lambert surface albedo. Reflected intensities were calculated using the isotropic surface albedo for the Haze L atmosphere and for wavelengths of 0.37μ and 0.54μ. The reflected intensities so obtained are compared with the reflected intensities obtained for the Lambert surface albedo, and are shown in Figs. 4 through 6. The reflected intensity in photons $m^{-2} sr^{-1}$ per source photon m^{-2} is plotted as a function of the cosine of the polar angle of reflection.

The data presented in these figures shows that the isotropic ground albedo model will underestimate the reflected intensity computed for the Lambert albedo model for cosines of the polar reflection angles from 1.0 (down) to approximately 0.77. After the cosine of the polar reflection angle decreases below 0.77, the isotropic ground albedo model will over-estimate the reflected intensity at the satellite position. This difference is independent of the magnitude of the surface albedo.

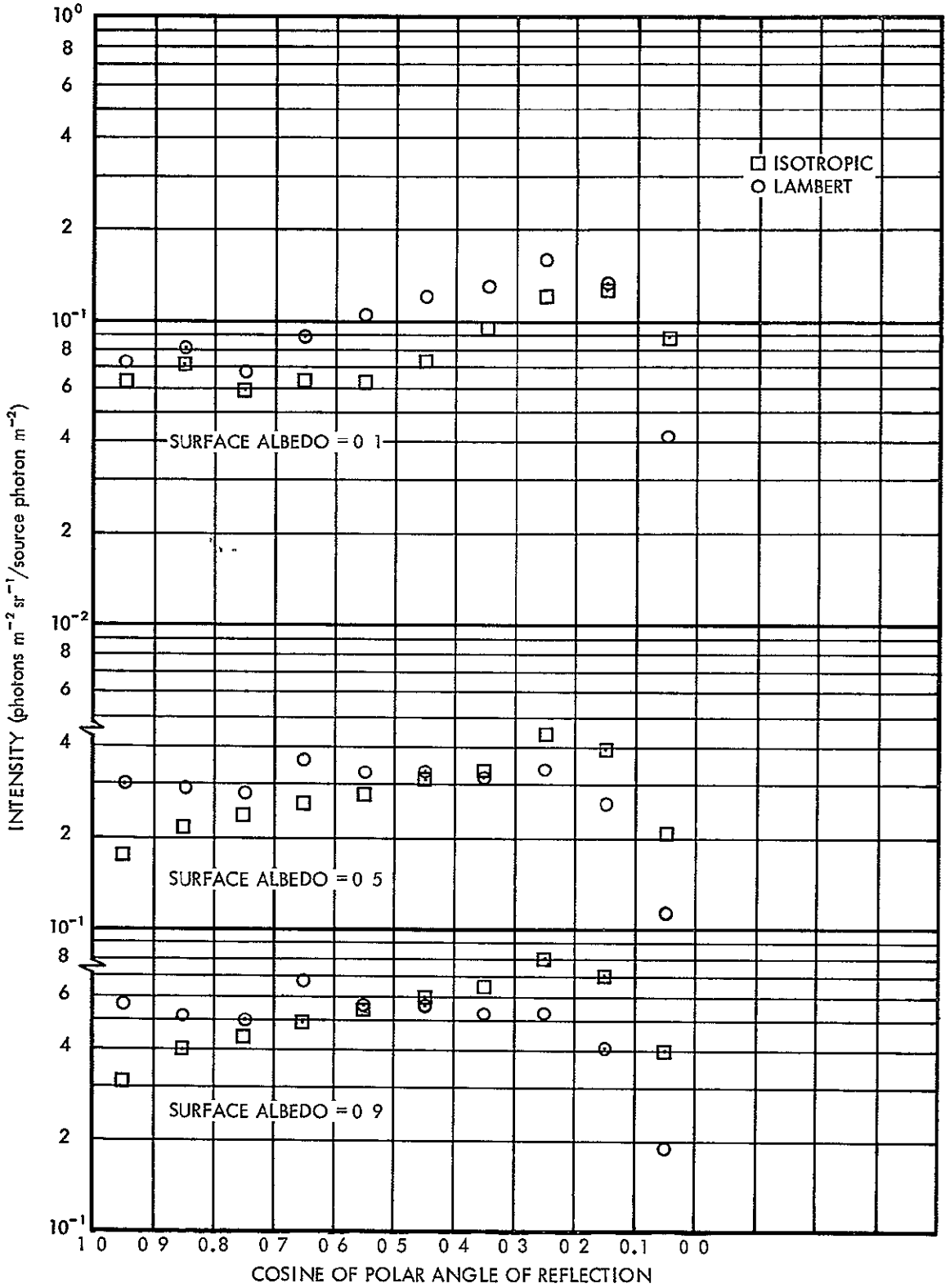

Fig. 4 Calculated Reflected Intensities for Cases where the Ground Surface is a Lambert or Isotropic Reflector $\lambda = 0\ 54, \mu_o \theta_o = 10^\circ$

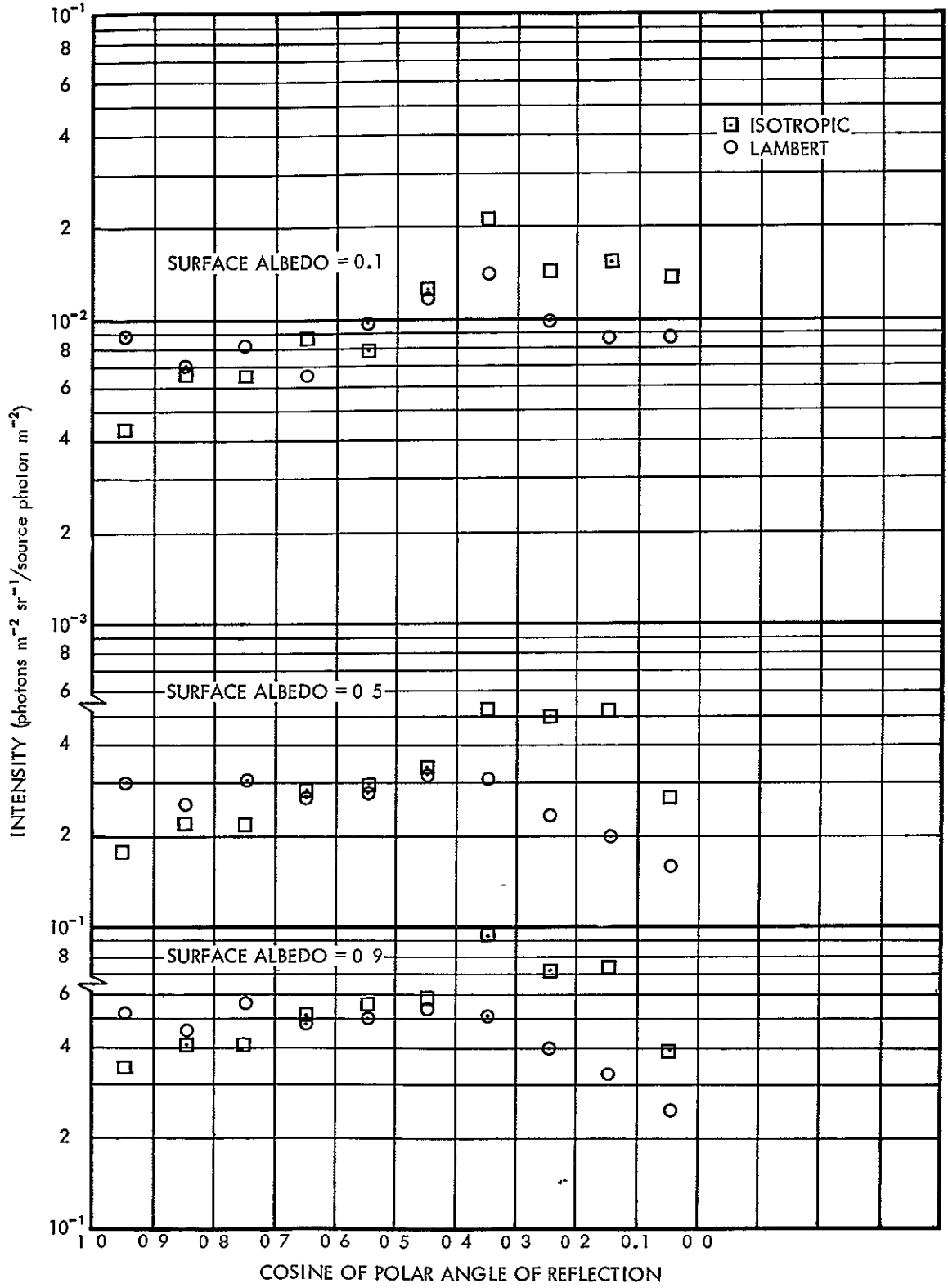

Fig 5 Calculated Reflected Intensities where the Ground Surface is a Lambert or Isotropic Reflector $\lambda = 0\ 54\mu$, $\theta_o = 40^\circ$

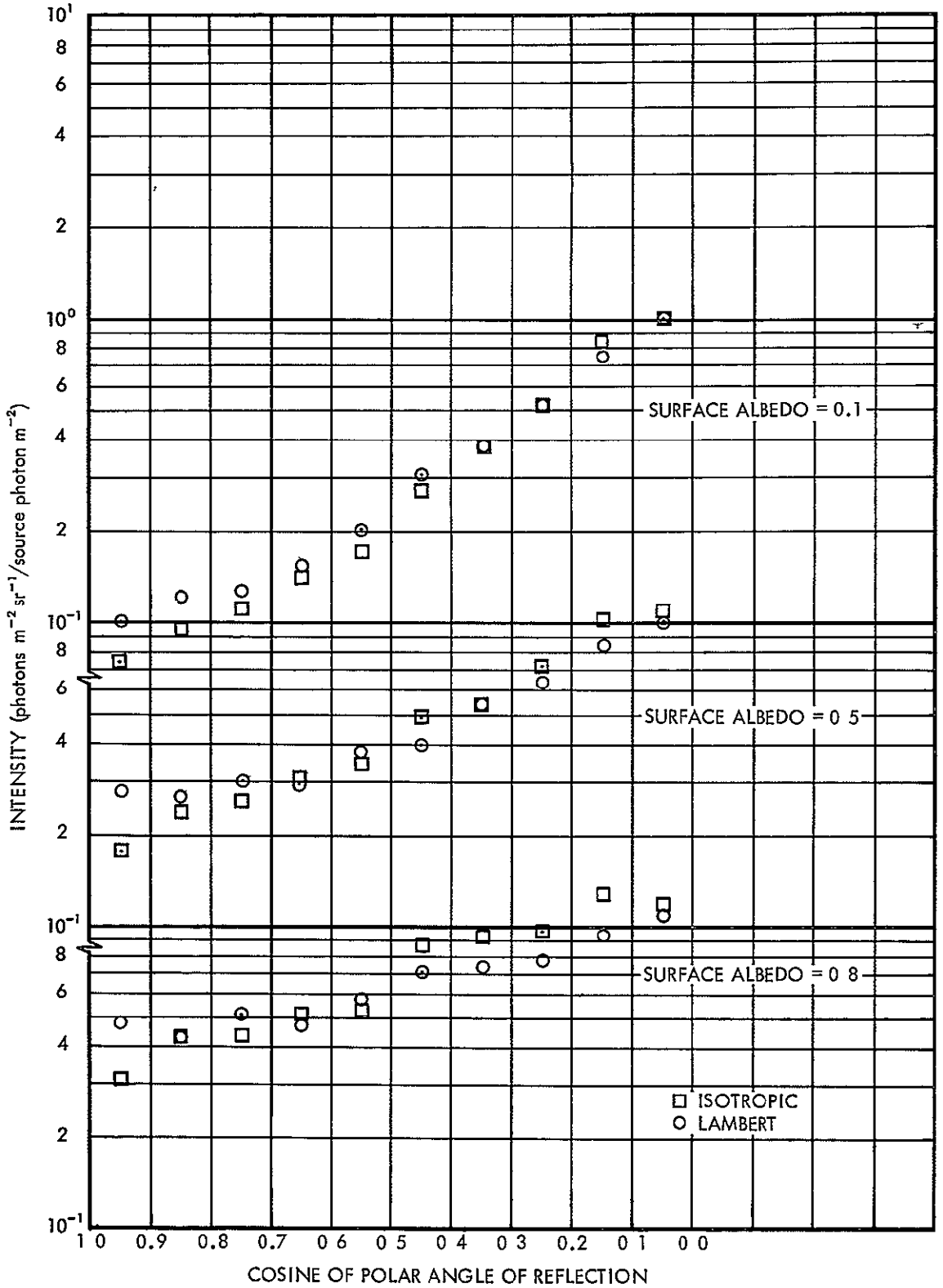

Fig 6 Calculated Reflected Intensities for Cases where the Ground Surface is a Lambert or Isotropic Reflector $\lambda = 0.54\mu$, $\theta_o = 70^\circ$

The differences are almost always 30% for small polar reflection angles with the isotropic ground albedo model lower, and 40% for cosines of the polar reflection angle less than ≈0.42, with the isotropic model yielding the higher reflected intensity estimates.

The Lambert surface albedo with the cosine type distribution function accounts for the greater number of photons that will be reflected in the forward direction, and hence is believed to give a more realistic calculation. The Lambert albedo calculations seem to be low for the large polar reflection angles. This is to be expected if one considers the geometry used for the model atmosphere. As will be shown later, the Monte Carlo calculations from a plane parallel atmosphere when compared with the OSO-III data were found to underestimate the reflected intensity for large polar view angles. An investigation of the experimental data indicates that the estimates of the reflected intensity obtained from the LITE-II calculation in which the Lambert surface albedo was used are low only for large incident angles and large polar view angles. Since these discrepancies are only observed over water, the underestimation is attributed to the situation where water becomes a Fresnel reflection rather than a Lambert reflection. If the general interest is only for large view angles and large incident angles, the isotropic surface albedo data may be used. However, for the general case we feel the Lambert model is more physically realistic. It should also be noted from Figs. 4, 5,

and 6 that as the solar incident angle increases, the estimate of the intensity for the isotropic surface albedo case is at most 10% greater than the estimate obtained when the ground surface was taken to be a Lambert reflector. It should also be noted that the magnitude of the ground albedo has little effect on the relative values of the reflected intensities for the two albedo models.

VI.. REFLECTED LIGHT AS A FUNCTION OF CLOUD MODEL

A study of three different cloud models was conducted to determine the effect of the cloud models on the calculated reflected intensities at the top of the atmosphere. The study was conducted for the 0.54μ wavelength with three different types of clouds. The cloud thicknesses were 0.1, 1.0, and 80 mean free paths. The 80 mean-free-path thick cloud was the model described in Ref. 66. The thinner clouds were based on the model of Deirmenjian (Ref. 4). LITE-II problems for these models were run for solar zenith angles of 10°, 40°, and 70°. The angular distributions for several of the six azimuth regions are shown in Figs. 7 through 9. The surface albedo for each case is 0.1.

For the solar incidence angle of 10°, shown in Fig. 7, the reflected intensity is independent of both the polar angle of reflection and the azimuth angle relative to the sun. The value of the reflected intensity increases as the cloud thickness increases, but by a much smaller fraction, i.e., the reflected intensities for the $\tau = 80$ cloud are approximately a factor of three larger than the reflected intensities from the cloud with $\tau = 0.1$. In all azimuth regions, the calculated reflected intensity values tend to be reduced in the polar reflection angle regions described by $\cos\theta$ less than 0.2. This reduction in the reflected intensity is due to the increased path length that the photon must traverse after being reflected from the earth's surface. For clouds with any optical

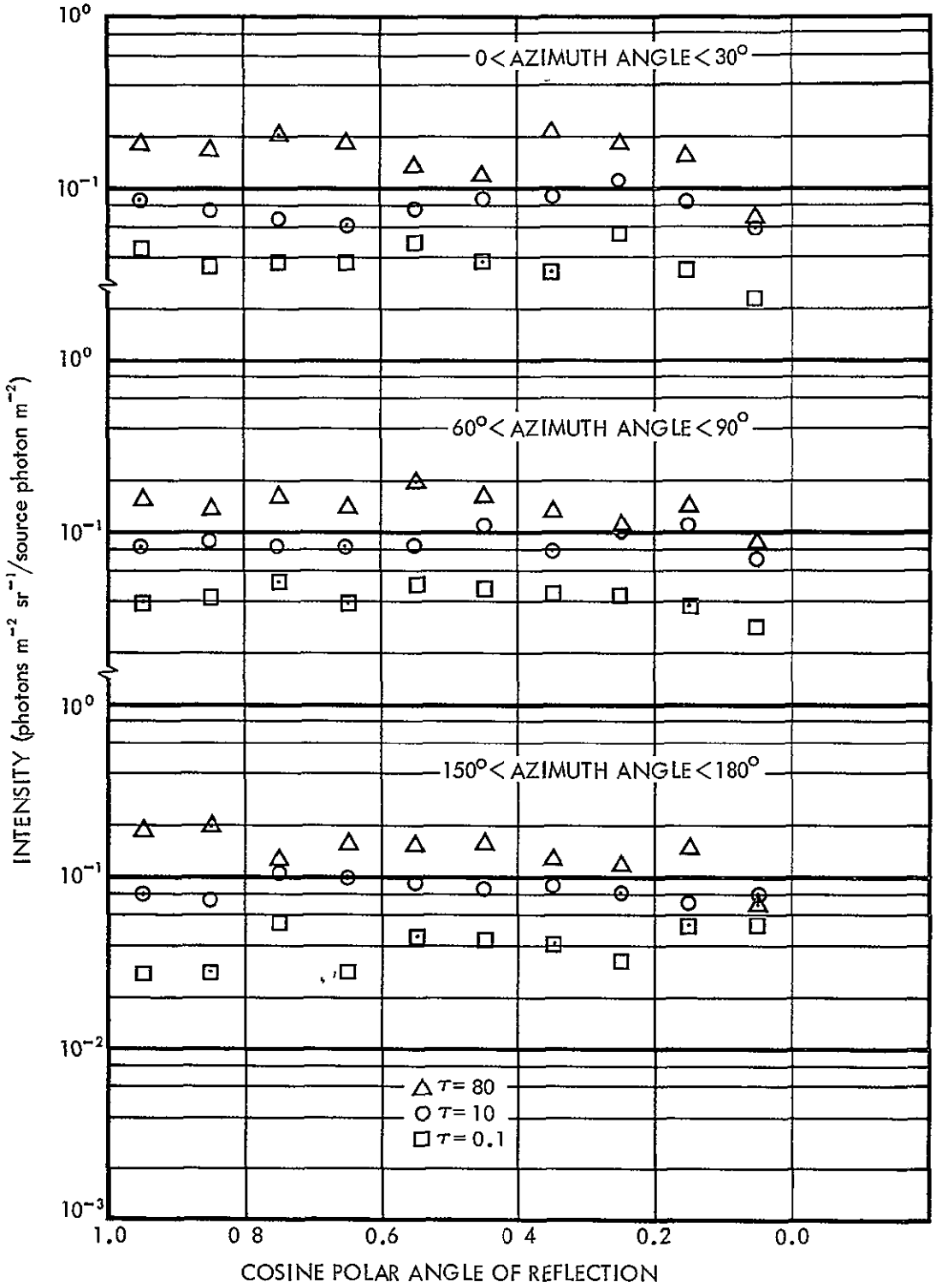

Fig. 7 Reflected Intensity as a Function of the Polar Angle of Reflection for Various Cloud Thicknesses $\lambda = 0.54\mu$, $\theta_o = 10^o$

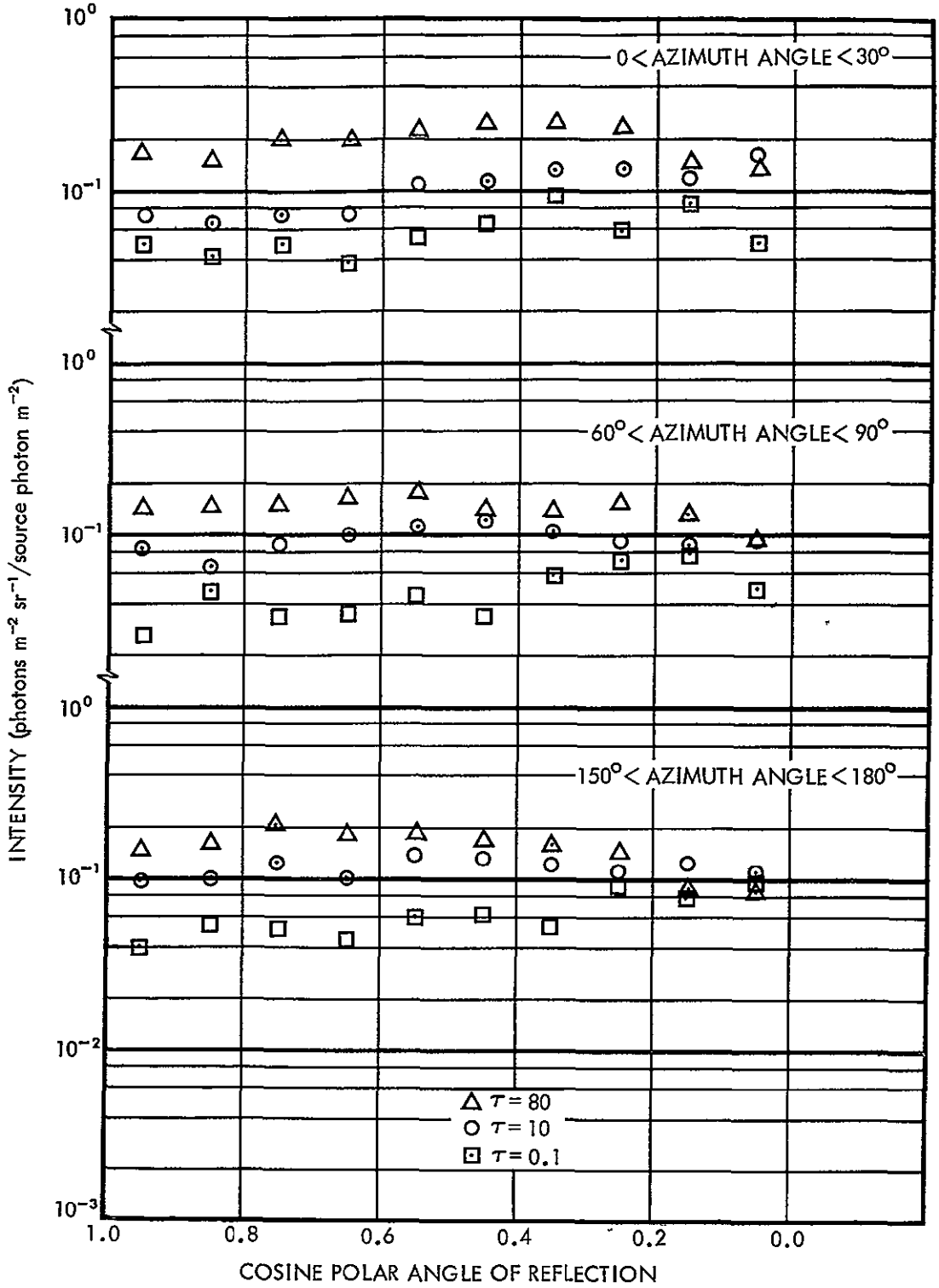

Fig. 8. Reflected Intensity as a Function of the Polar Angle of Reflection for Various Cloud Thicknesses $\lambda = 0.54\mu$, $\theta_o = 40°$

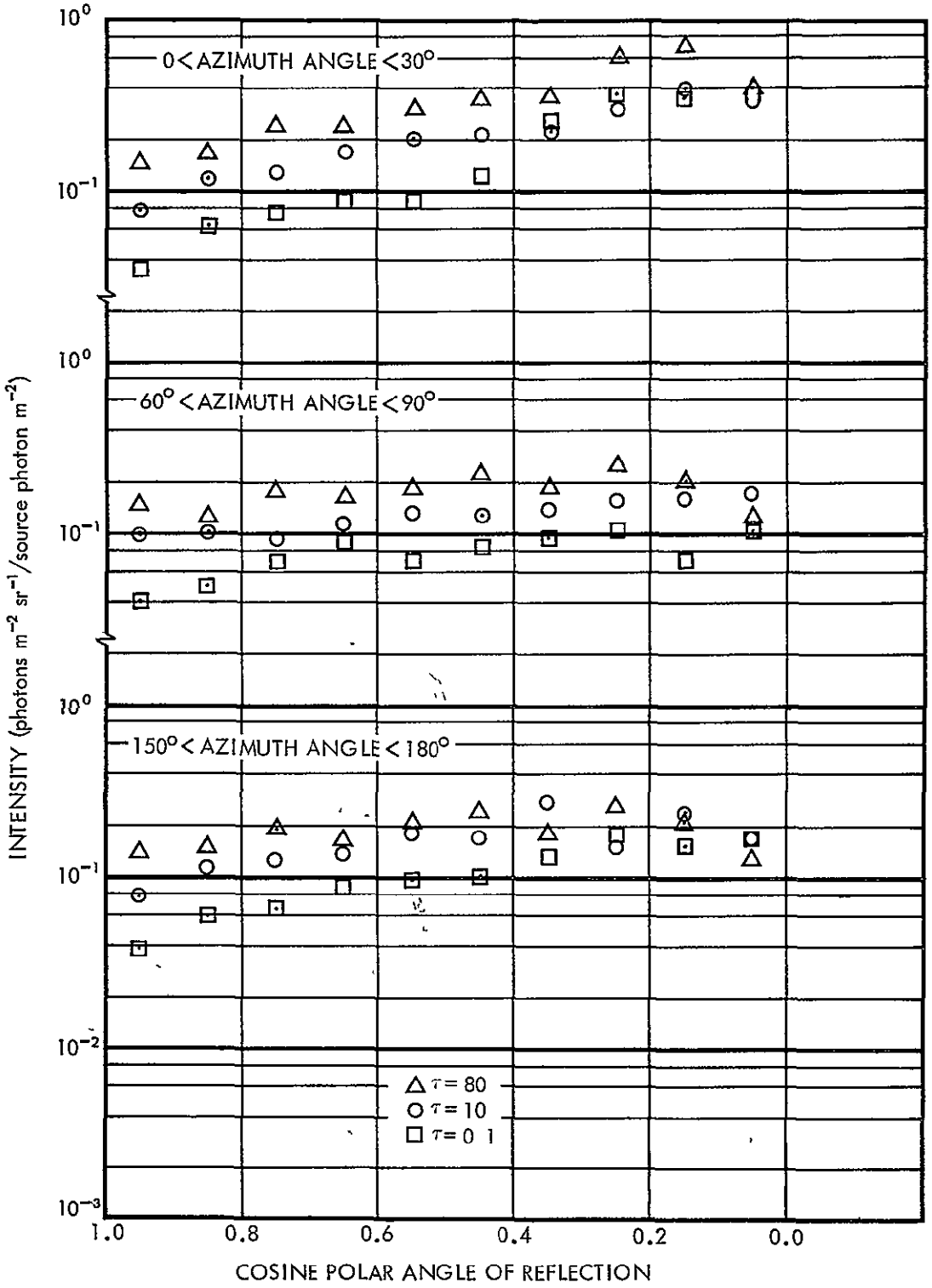

Fig 9 Reflected Intensity as a Function of the Polar Angle of Reflection for Various Cloud Thicknesses $\lambda = 0.54\mu$, $\theta_o = 70°$

thickness, these photons will be unable to penetrate the cloud at these longer path lengths.

The data presented in Fig. 8 for the solar zenith angle of 40° shows a somewhat different angular distribution. There is some statistical variation in this data; however, it is evident that the calculated reflected intensity shows a minimum for cosθ approximately equal to one, and a maximum for the smaller cosine values. This variation is more pronounced with the optically thin clouds. The variation for the $\tau = 80$ cloud is not as great, but a definite slope can be seen. For this model, the reduced value for the intensity for long path lengths can again be seen in the cosine regions 0.0 to 0.1 and 0.1 to 0.2. This set of data shows clearly the effects of multiple scattering. For the $\tau = 0.1$ cloud, the variation as a function of the polar angle is a maximum for small cosθ values as expected from the single scattering phase function. For the $\tau = 1.0$ cloud the multiple scattering effects become more important, and the intensity is nearly the same, with a slight slope, increasing as the number of single scattering centers in the line of sight increases. The very thick cloud with $\tau = 80$ shows even less variation with polar angle and also shows the reduced probability of a photon traversing the cloud at a large angle, indicating a longer path length.

The data shown in Fig. 9 are for a solar zenith angle of 70°. This data shows the greatest polar angular variation. The intensity for this case is largest for the small values of the cosine of the

angle of reflection, and falls regularly to a minimum near the zenith. The variation is greatest for the thin clouds, and is reduced by multiple scattering for the thick cloud. This can be understood in terms of the path that a photon follows upon entering the cloud. When the sun is overhead, the photons efficiently penetrate the cloud with a large number of small angle forward scatterings. The probability of a photon undergoing backscattering is small, and if backscattering does occur, the long optical path back through the cloud reduces its contribution to the reflected intensity at the top of the atmosphere. For a large angle of incidence, the photon will travel approximately the same distance with a large number of small angle forward scatterings. These photons may scatter out of the cloud with a smaller scattering angle then the photons in the case of overhead sun. This smaller scattering angle is more probable than backscattering, and the optical distance to the top of the cloud is smaller. The higher probability of scattering increases the reflected intensity in terms of the number of photons reaching the top of the atmosphere, and the shorter optical path increases the contribution to the reflected intensity by each photon.

The data presented in this study can be compared in a general sense with the TIROS-IV data (Ref. 8). The TIROS data is not monochromatic but spans a wavelength range of 0.55μ to 0.75μ, and is averaged over several clouds. The data of Fig. 6 of Ref. 8 is compared with the LITE-II data in Table I. The measured and calculated intensity for

each polar and azimuth region has been normalized to the data for a polar cosine of 0.8. The comparison of the two sets of data in Table I indicates that the LITE-II calculations have the same functional form as the TIROS measurements.

Other measurements that indicate these calculations are representative of the physical situation are reported in Ref. 13. Figure 26 of Ref. 13 shows the bidirectional reflectance measured at an altitude of 25,000 ft., from a 2500 ft. thick stratocumulus cloud over the Pacific ocean. The solar zenith is 72.2° with an azimuth of 45°. This data may be compared with the data shown in Fig. 9. The general shape and the relative values of the maximum and minimum agree quite well. Both the calculated intensities and the measured intensities reported in Fig. 26 of Ref. 13 were normalized to their respective values, at a polar cosine equal to 1.0. A comparison of the normalized measured and calculated intensities is shown in Table II. The aircraft measurements indicate a change of intensity by a factor of three with polar angle while our calculations show a difference of approximately four for $\tau = 80$. The aircraft measurements show a maximum at a polar view angle of 75° while the LITE-II calculations show a maximum between 70° and 80°. When the calculated values were compared with measurements from this same cloud (Fig. 29, Ref. 13) for an azimuthal angle of reflection of 135°, very good agreement was noted. For that azimuthal angle the ratio of the aircraft measurements of the intensity at a polar reflection angle of 0° to the maximum

Table I. Comparison of the Intensities Calculated by LITE-II for a stratus Cloud with Measured Values from TIROS-IV

Cosine of Polar Angle of Reflection	Azimuthal Angle Interval 0-30°		60-90°		150-180°	
	TIROS	LITE-II	TIROS	LITE-II	TIROS	LITE-II
0.80	1.0	1.0	1.0	1.0	1.0	1.0
0.50	1.53	1.5	1.1	1.17	1.2	1.3
0.00	1.69	1.7	1.1	0.88	1.2	1.25

Table II. Comparison of LITE-II Calculations with Aircraft Measurements for a Stratus Type Cloud: θ_o=70.2°, ϕ=45°, τ=80

Cosine Polar Angle of Reflection	LITE-II	Measured Data (Ref. 13)
1.0	1.00	1.50
0.9	1.13	1.06
0.8	1.59	1.30
0.7	1.59	1.64
0.6	2.00	2.00
0.5	2.33	2.37
0.4	2.46	2.72
0.3	3.99	2.90
0.2	3.67	2.70
0.1	2.66	2.30

value is 1.5. The ratios of the maximum to minimum calculated values from Fig. 9 is 1.6. One should also note for the 135° azimuthal angle that in both the measured and calculated cases the maximum value of the intensity has been shifted down by five degrees to a polar view angle of 70°.

VII. COMPARISON WITH EXPERIMENTAL DATA

The validity of any calculation method depends on its ability to predict experimental data. A primary task was to determine how well the Monte Carlo calculated data predict the data taken by the albedo experiment on OSO-III. This data was made available in physical units on magnetic tape. Due to the large quantity of data a computer program was written to compare the measured data with the calculated intensities from LITE-II.

The albedo data on tape is in physical units, nwatt/cm^2-Å-sr. To compare this data with the Monte Carlo calculations it is necessary to normalize the measured data with the solar spectrum. The solar spectrum (Ref. 9) used to normalize the raw data is given in Table III. The raw data was normalized

Table III. Solar Energy Incident to the Top of the Atmosphere at the OSO-III Wavelengths.

Wavelength (microns)	Solar Constant (nwatts/cm^2-Å)
0.37	13,320.0
0.45	21,442.0
0.54	19,800.0
0.67	15,520.0
0.78	11,835.0

by using the solar constant $I_o(\lambda)$ and the incident angle θ_o. The

value used for comparison with the Monte Carlo calculations is

$$I_L(\lambda) = \frac{I_m(\lambda)}{I_o(\lambda)\mathrm{Cos}_o}$$

where $I_o(\lambda)$ is the measured data in nwatts/cm^2-Å-sr. The quantity $I_L(\lambda)$ is now in units of photons/m^2-sr per source photon/m^2, the units of the LITE-II calculation.

The raw data was sorted first on wavelength, and then stored on magnetic tape in order of increasing solar zenith angle. The geometric parameters taken from the OSO-III experiments are different from parameters used in the calculations, and hence a number of transformations were necessary before a comparison could be made. The geometry of the satellite is shown in Fig. 10, with the LITE-II geometry shown in Fig. 1. The data retained by the OSO-III experimentor are sufficient to determine these transformations.

It is first necessary to determine the subsolar point for a given measurement. Since the data contains the orbit number and the time of the measurement, the subsolar point may be determined emperically rather quickly by

solar latitude = -4.46 + (orbit number - 20.0) 1.57/651.0

solar longitude = 180.0 - (GMT)/240.0 .

The subsolar point for a given measurement is identified by SOLA, SOLO for latitude and longitude respectively. Three other quantities necessary for the comparison require several secondary calcu-

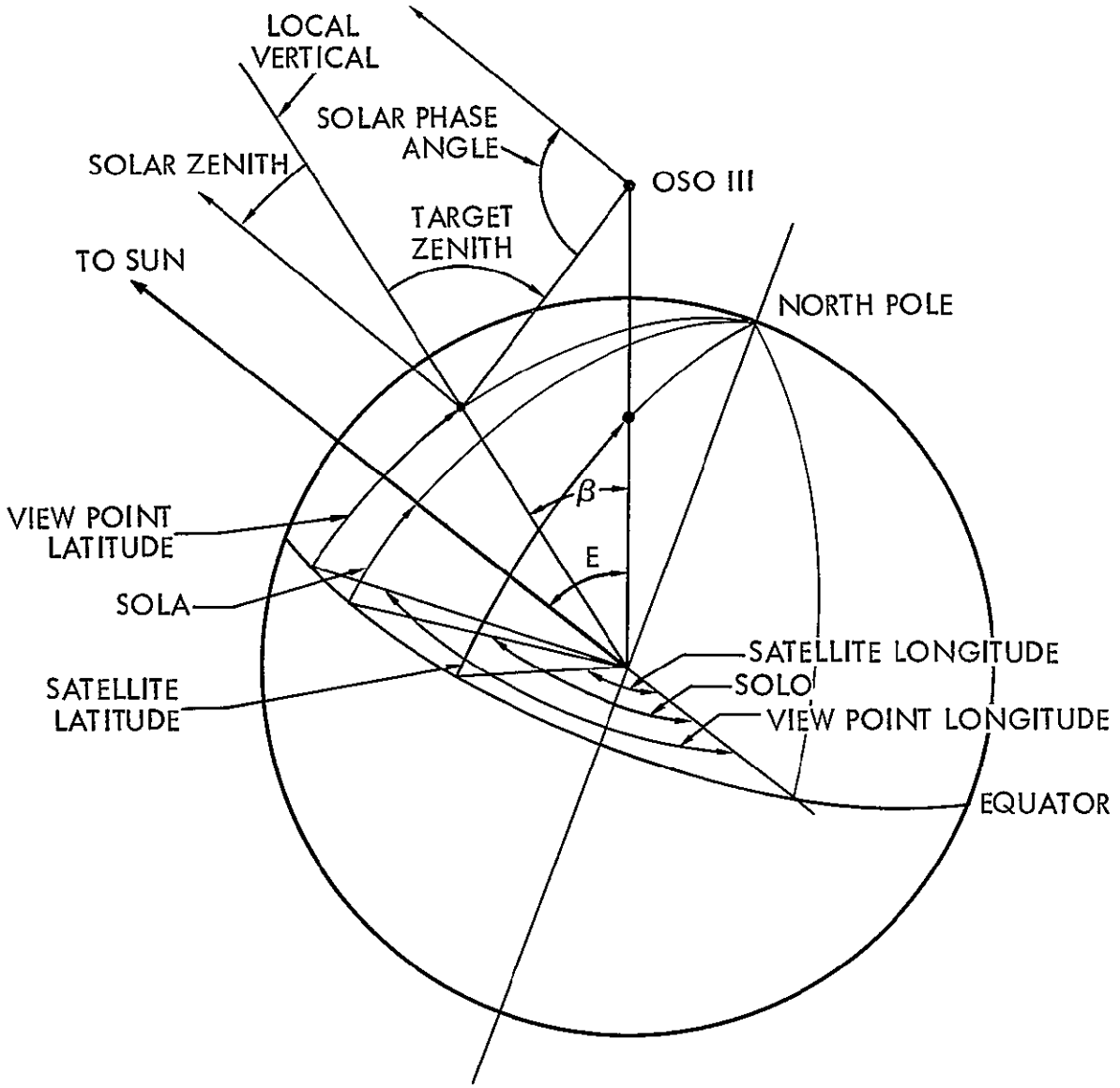

Fig. 10. Satellite-Sun-View Point Geometry

lations. These quantities are: solar angle of reflection, azimuth angle relative to the sun, and the angle at the center of the earth between the radius to the satellite and the radius to the subsolar point. These parameters are calculated as follows.

Let B represent the angle at the center of the earth between the radius vector to the satellite and the radius vector to the view point; then with the use of spherical triangles the cosine of B may be calculated by

COSB = cos(90.0° -satellite latitude)*cos(90.0°- view point latitude)
+ sin(90.0° - satellite latitude)*sin(90.0° - view point latitude)
* cos(satellite longitude - view point longitude).

The cosine of the earth angle may be calculated by

COSE = cos(90.0° - satellite latitude)*cos(90.0°-SOLA)
+ sin (90.0° - satellite latitude)*sin(90.0°-SOLA)
*cos(satellite longitude-SOLO).

Using the above values, the polar cosine of reflection, and the azimuth angle relative to the sun may be calculated. The cosine of the azimuth angle relative to the sun is

CPH = (cos(solar zenith angle)*cos(target zenith angle)
-cos(180.0°-solar phase angle))/sin(solar phase angle)
*sin(solar zenith angle).

The cosine of the polar angle of reflection is calculated by

CPOL = cos(target zenith angle - B).

The calculated values that are to be compared with the experimental data are for a single model atmosphere, therefore one must test the view point to determine the type of atmosphere model that is suitable. To accomplish this, the area between latitude 35°N and 35°S was divided into 5° intervals. These intervals are then followed completely around the world to determine what sections will be land masses. A world map of IF tests was constructed to determine the type of surface one would see for a particular view point latitude and longitude. If the surface is not of the type described by the atmosphere model, the measurement is rejected and a new measurement is read into the computer. When the correct type of surface is found, the code calculates the necessary angles described earlier, and then performs a search of the LITE-II data to determine the calculated intensity that most nearly represents the measured value.

The calculated intensities are for a single incident angle, hence it is necessary to divide the measured values into groups determined by the incident solar radiation. The measurements made for an incident angle less than five degrees are compared with the calculated data with incidence solar angle equal zero degrees, etc. The incidence angle intervals, and the incident angle used for the calculations are shown in Table IV.

Table IV. Discrete Angles Used for Various Zenith Angle Ranges of the Incident Radiation.

Measured Data (degrees)	LITE-II Incident Angle (degrees)
0-5	0.0
5-15	10.0
15-25	20.0
25-35	30.0
35-45	40.0
45-55	50.0
55-65	60.0
65-75	70 0
75-82	80.0
82-90	85.0

The comparisons for a wavelength of 0.67μ with the clear Haze M model are displayed in Figs. 11 through 13. These figures show a comparison of the measurements over water with calculated data for a clear maritime atmospheric condition. The large quantity of the data makes it impossible to display all of the measured data, hence these graphs contain only a representative sample. It should also be noted that the measurements tend to fall within particular polar and azimuth angle regions. This is not surprising when one considers the experimental set up (Ref. 10). The sun oriented spacecraft will make measurements in certain azimuth and polar regions on every other revolution, for each wavelength.

All of the measured data for a solar angle of incidence less than 5° and a wavelength of 0.67μ are compared in Fig. 11 with the calculated data for a clear maritime atmosphere. The Monte Carlo data plotted in Fig. 11 are for cases where the surface albedos are either 0.1 or 0.2. The measurements were taken over water, and hence, as expected, are seen to have a low albedo. Most measurements compare well with the Monte Carlo calculations for a surface albedo of 0.1, the approximate value expected.

The sample of data shown in Fig. 12 is the measured and calculated data over water for a wavelength of 0.67μ with the solar incidence angle between 25.0° and 35.0°. The Monte Carlo data is for a solar angle of incidence of 30.0°. The sample of experimental points shown represents approximately the number of measurements found to fall within each angle region.

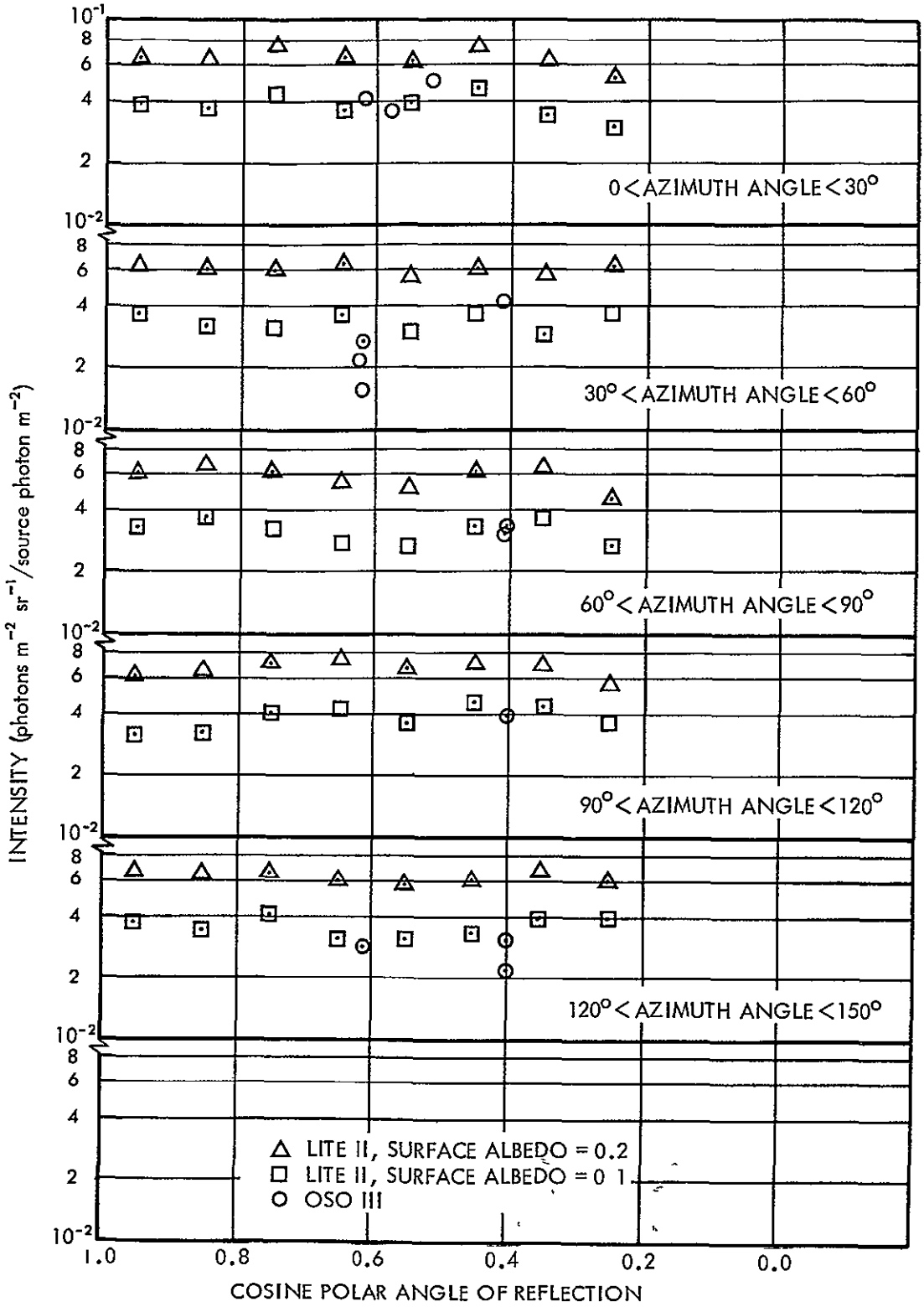

Fig. 11 Comparison of Measured and Calculated Reflected Intensities for a Maritime Atmosphere $\lambda = 0.67\mu$, $\theta_o \cong 0°$

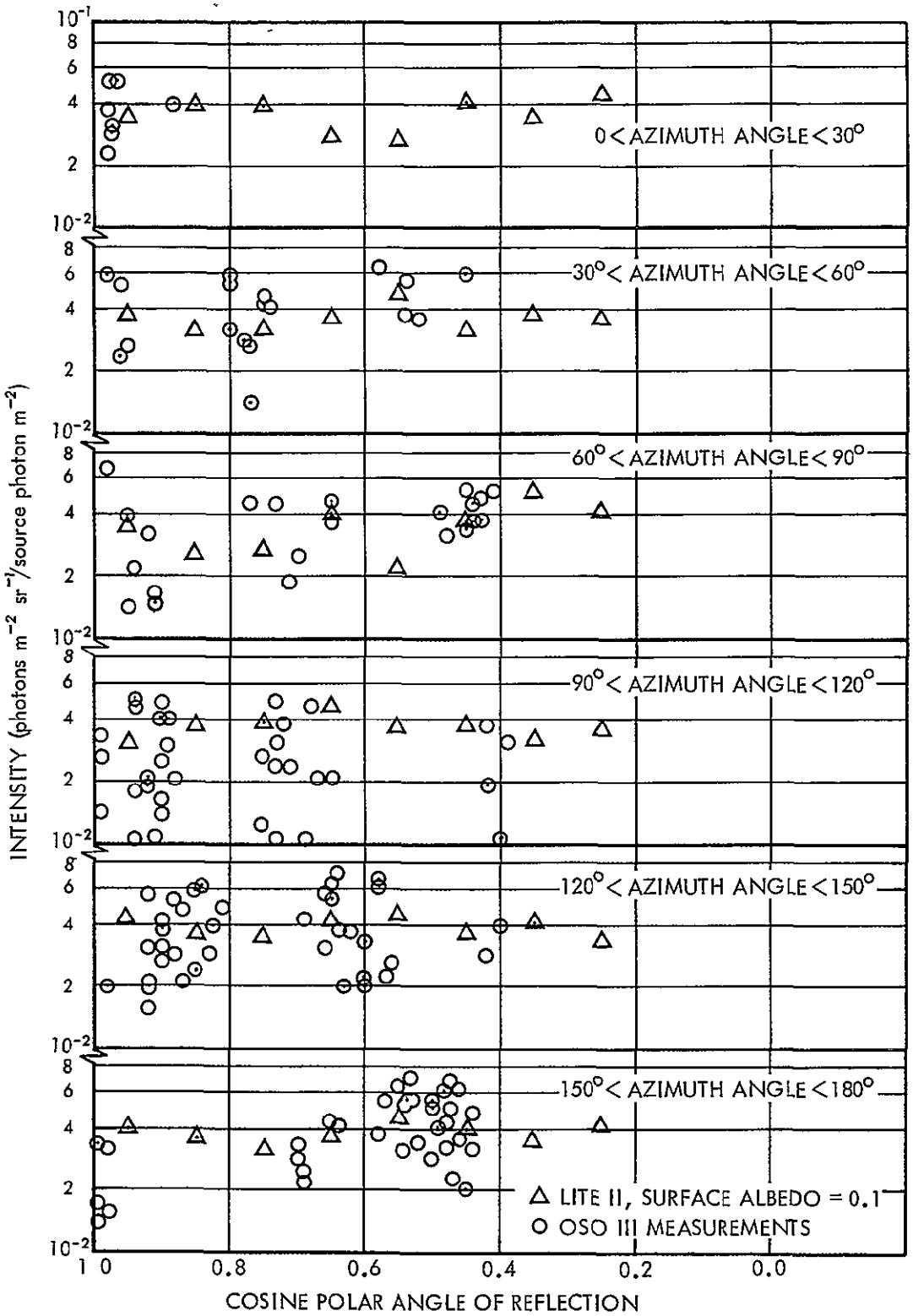

Fig 12. Comparison of Measured and Calculated Reflected Intensities for a Maritime Atmosphere $\lambda = 0.67\mu$, $\theta_o = 30°$

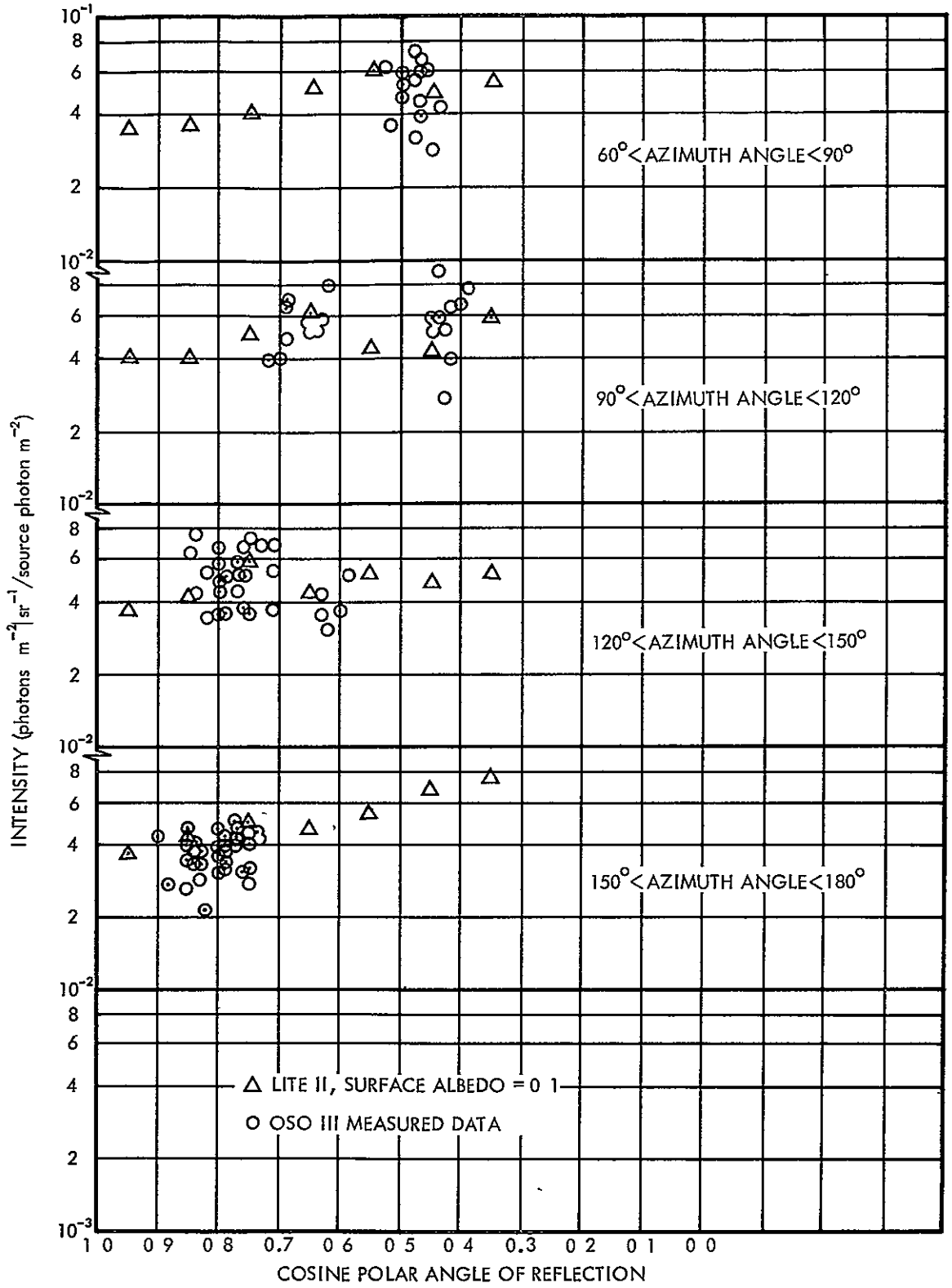

Fig 13 Comparison of Measured and Calculated Reflected Intensities for a Maritime Atmosphere $\lambda = 0\ 67\mu$, $\theta_o \cong 60^\circ$

The Monte Carlo calculations shown in Fig. 12 assumed the surface albedo to be 0.1. In general the measured data is near the calculated value, indicating a surface albedo of near 10%. None of the measurements above the calculated value for the 0.1 surface albedo approach the value calculated for a surface albedo of 0.2. In the azimuth regions defined by the azimuth angles 90° to 120° and 150° to 180° there are several data points that are somewhat lower than the calculated data. These low intensity values are greater than the calculated value for a ground albedo of 0.0. If a sample exponential extrapolation is performed from our Monte Carlo calculations, the lower measured points yield an albedo near 5%.

Investigation of the complete set of measured data shows that the measured values are for low surface albedos that have the same range as the sample of calculated data shown in Fig. 12. This variation is due to the changing atmospheric and surface conditions. The calculated values are for a single albedo and a single model atmosphere, and should represent the intensity observed only for these surface conditions. The data shown in Fig. 12 for azimuth regions of 30° to 60° and 60° to 90° are a particularly good example of the type of comparisons one could get for known atmospheric and surface conditions.

The measured data for all other incident angle groups below 80° show approximatley the same fit to the calculated data, with the same variation. A sample of the measured data and calculated estimates

for the incident polar angle group of 55° to 65° is shown in Fig. 13 for comparison.

The one serious exception to the rather good agreement between the measured and calculated data is data taken with low sun, and large polar view angles All of the OSO-III data taken over water with solar zenith angles greater than 82° was with a polar view angle greater than 50°. The intensity values measured in this case are approximately a factor of three over the values measured for other incident angles. With the large angle of incidence and the large polar reflection angle, the Lambert type surface, used in our calculations, is not a good approximation for water. The fact that water becomes a Fresnel type reflector accounts for the higher value of the observed intensity.

In a comparison of this type it is impossible to determine whether the view point is clear or cloudy. After the comparisons have been made it is possible to check the view points which show a high albedo with the ESSA photographs. Such a spot check indicates that the measured data which are for an albedo greater than 0.5 are for view point regions covered with clouds. A sample of the cloud data for a solar incident angle of 20° is shown in Fig. 14. The angular distribution for the case is rather flat for all polar and azimuth regions. There are fourteen experimental points that fall above the value estimated for the atmospheric model containing an 80 mean-free-path thick stratus cloud. In general the Monte Carlo calculations tend to overestimate the experimental values. The

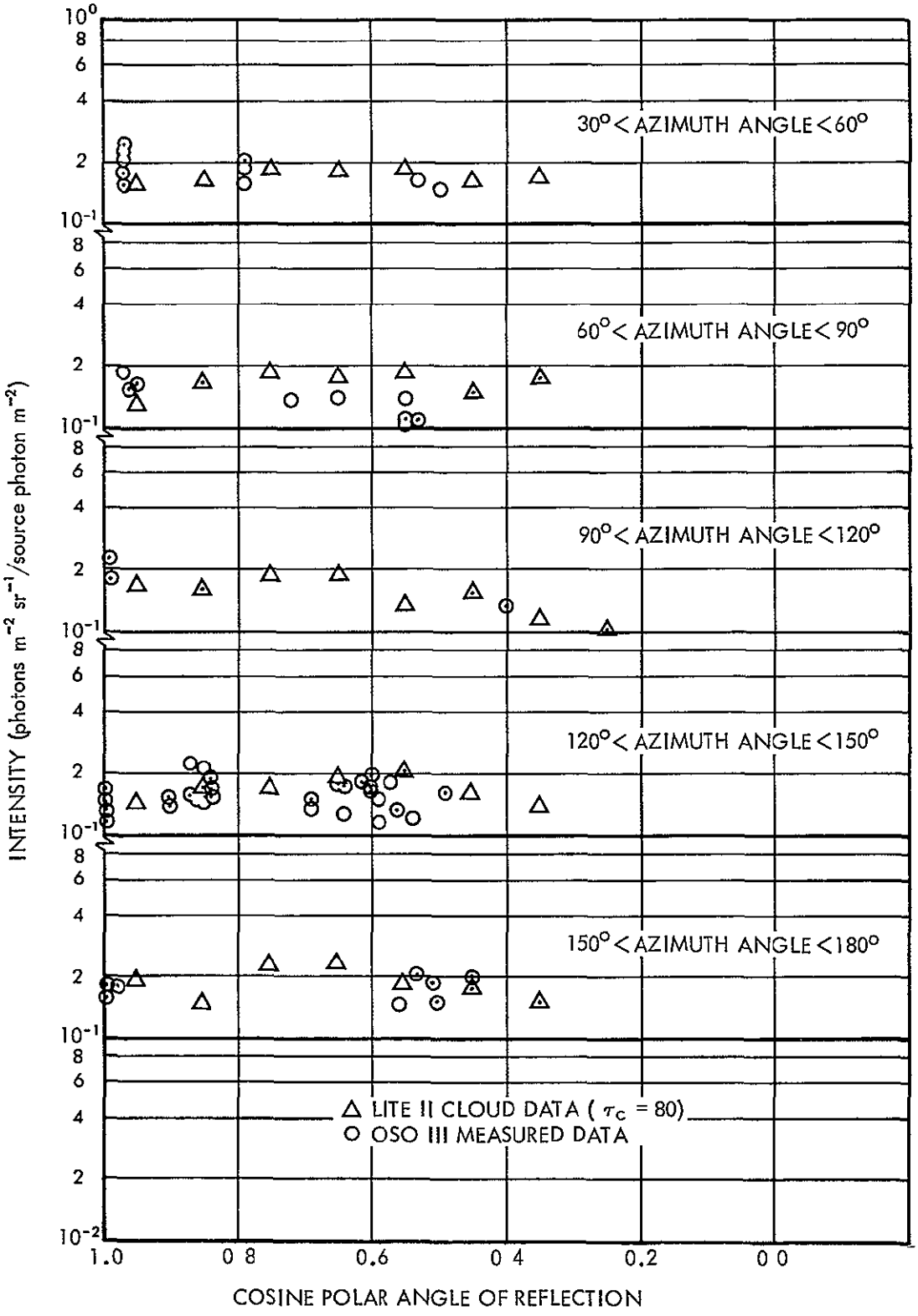

Fig 14. Comparison of Measured and Calculated Reflected Intensities for a Maritime Atmosphere with a Stratus Cloud $\lambda = 0.67\mu$, $\theta_o \cong 20^o$

larger value calculated by the Monte Carlo method is to be expected since we have assumed the single scattering albedo to be 1. For clouds of this thickness (80 mean-free-paths), Ref. 12 indicates that the single scattering albedo is approximately 0.993. If the single scattering albedo is reduced to this value, the intensity estimates would be reduced by 40 to 50%, yielding values below the bulk of the experimental values. The value of the single scattering albedo in Ref. 12, which was obtained from the data of Ref. 11, seems to be high for the data we have. Water droplets having a diameter of a few microns should have a value of the single scattering albedo near unity. The differences observed between the experimental values and the calculated values imply that the dust or salt particles on which the water condensed has a marked effect on the single scattering albedo. The somewhat higher single scattering albedo that we have estimated is probably due to the fact that these measurements over the ocean with salt as the principle condensation nuclei, would yield a higher single scattering albedo than would the aerosols observed over land.

It is expected that the single scattering albedo will vary from place to place depending on the local variation of the aerosol content. For a more accurate calculation a reasonable estimate of this albedo should be made. If experimental measurements are available, the Monte Carlo calculations are quite useful for obtaining the estimate.

All OSO-III measurements made available to us were compared to the LITE-II calculations. The comparison were divided into two areas, measurements over the ocean and measurements over land. As stated earlier the high albedo measurements agree rather well with the cloud calculations, therefore these comparisons will be made only with the Monte Carlo data for the maritime Haze M and for the continental Haze L.

There were 41,697 OSO-III measurements taken over the ocean. These measurements were compared with the clear Haze M calculations. When an experimental value for the intensity is compared with the LITE-II data, the only way it may be rejected is for the experimental value to be larger than the largest LITE-II value, (α=0.9) or smaller than the smallest LITE-II value (α=0.0). Of the OSO-III samples over water, there were approximately 7.5% (3137) of the measurements below the smallest value calculated by LITE-II. Only 0.6% (239) of the measurements were above the largest value calculated by LITE-II, thus leaving approximately 92% of the available measurements that were compared with the LITE-II calculations. Investigation of the data indicates that most of the measurements which were above the value computed by LITE-II for a surface albedo of 0.9 occur for large solar zenith angles where water is no longer a nearly Lambert surface. The few measurements that exceeded the calculated data for a surface albedo of 0.9 at small solar zenith angles are probably due to spectral reflection, which is not treated in these calculations or the calculations for heavy cloud cover. The measurements with values

less than the smallest value of the LITE-II calculations probably indicate that the atmosphere covering these areas had a ground level meteorological range greater than 25 km.

A summary of the comparisons of the measurements made over the ocean is given in Tables V through IX. In these tables all measurements yielding a surface albedo greater than 0.5 was assumed to be clouds, and reported as a single unit. If one considers the gross trends of this data, the shift (in percentage) of measurements toward the higher albedos as the solar zenith angle increases is evident. It is also noted that the bulk of the measurements for the three longer wavelengths have shifted toward the lower albedos with the maximum shift in the 0.78μ data. If one looks at a specific sample of the data as shown in Table X, the general type of comparison can be seen. The data shown in Table X are for $\theta_o \simeq 30°$, $\cos\theta \simeq 0.64$, and $\cos\phi \simeq -0.56$ and are from orbit 35 at a satellite position of 24°N., 173°E. The surface albedo for a water surface usually ranges from about 0.15 to 0.2 for wavelengths between 0.37μ and 0.78μ. The albedo ranges indicated in Table X for a water surface agree reasonably well with the accepted values for wavelengths of 0.54μ, 0.67μ, and 0.78μ. The surface albedos for water of just slightly over 20% as indicated by the comparison between the LITE-II and OSO-III data in Table X for $\lambda=0.37\mu$ and $\lambda=0.45\mu$ are slightly higher than the usually accepted values for those wavelengths.

Table V. Number of OSO-III Measurements which Lie in Indicated Ground Albedo Ranges When Compared with the LITE-II Data for a Maritime Atmosphere: λ=0.37μ

Incident Solar Angle (deg)	Ground Albedo Range						Total
	0.0-0.1	0.1-0.2	0.2-0.3	0.3-0.4	0.4-0.5	>0.5	
0	4	6	3	2			15
10	28	149	134	61	28	46	446
20	141	593	525	208	76	50	1593
30	174	536	385	270	133	154	1652
40	115	342	363	248	158	151	1377
50	80	230	251	166	188	262	1177
60	30	113	185	205	211	296	1050
70	23	45	74	87	284	255	622
80	3	2	1	10	24	56	96

Table VI. Number of OSO-III Measurements which Lie in Indicated Ground Albedo Ranges When Compared with the LITE-II Data for a Maritime Atmosphere: $\lambda=0.45\mu$

Incident Solar Angle (deg)	Ground Albedo Range						Total
	0.0-0.1	0.1-0.2	0.2-0.3	0.3-0.4	0.4-0.5	>0.5	
0	5	7	2				14
10	118	191	75	40	22	14	459
20	553	660	229	66	36	16	1560
30	540	452	356	170	69	67	1654
40	444	371	272	136	49	60	1342
50	143	302	219	171	112	155	1121
60	158	217	186	144	118	146	969
70	84	107	125	118	91	109	634
80	8	11	25	28	32	27	131
85		2		5	14	29	50

Table VII. Number of OSO-III Measurements which Lie in Indicated Ground Albedo Ranges When Compared with the LITE-II Data for a Maritime Atmosphere. $\lambda=0.54\mu$

Incident Solar Angle (deg)	Ground Albedo Range						Total
	0.0-0.1	0.1-0.2	0.2-0.3	0.3-0.4	0.4-0.5	> 0.5	
0	9	4					13
10	137	189	90	31	20	18	485
20	733	505	188	69	40	18	1553
30	564	501	288	147	71	62	1633
40	467	343	287	165	80	73	1415
50	242	297	204	157	123	177	1200
60	115	228	199	169	150	165	1026
70	35	85	115	124	126	172	657
80	5	8	11	20	15	50	119
85				1		18	27

Table VIII. Number of OSO-III Measurements which Lie in Indicated Ground Albedo Ranges When Compared with the LITE-II Data for a Maritime Atmosphere·λ =0.67μ

Incident Solar Angle (deg)	Ground Albedo Range						Total
	0.0-0.1	0.1-0.2	0.2-0.3	0.3-0.4	0.4-0.5	>0.5	
0	10	3					13
10	216	155	66	26	14	9	486
20	853	476	146	50	24	10	1559
30	772	436	192	111	34	44	1589
40	585	362	186	104	18	37	1332
50	331	274	232	128	94	102	1161
60	211	223	187	154	107	91	973
70	101	140	118	109	70	101	639
80	16	18	25	37	8	24	138
85		3	10	13	13	21	60

Table IX. Number of OSO-III Measurements Which Lie in Indicated Ground Albedo Ranges When Compared with the LITE-II Data for a Maritime Atmosphere: $\lambda=0.78\mu$

Incident Solar Angle (deg)	Ground Albedo Range						Total
	0.0-0.1	0.1-0.2	0.2-0.3	0.3-0.4	0.4-0.5	>0.5	
0	15	0	2				17
10	261	114	40	17	8		440
20	886	238	62	19	9	9	1225
30	668	369	127	38	33	7	1242
40	506	285	131	48	29	3	1002
50	374	208	171	107	46	16	922
60	296	231	149	106	44	17	843
70	163	131	99	82	54	9	536
80	23	16	13	9	3	0	64
85	9	4	4	1	0		19

Table X. Comparison of OSO-III and LITE-II Intensities for a Maritime Atmosphere: $\theta_o \simeq 30°$, $\cos\theta \simeq 0.64$, $\cos\phi \simeq -0.56$

Wavelength (μ)	Intensity (photons m^{-2}/source photon m^{-2})				
	LITE-II Data				OSO-III Data
	Albedo	Intensity	Albedo	Intensity	
0.37	0.3	1.45-01	0.2	1.26-01	1.33-01
0.45	0.3	1.25-01	0.2	9.40-02	9.60-02
0.54	0.2	8.27-02	0.1	6.15-02	7.48-02
0.67	0.2	7.40-02	0.1	4.30-02	4.80-02
0.78	0.1	4.35-02	0.0	1.30-03	3.08-02

There were 28,983 OSO-III measurements in the data sample from land masses. These data were compared with the LITE-II calculations for the continental Haze L model atmosphere. The summary of the number of measurements in each albedo range is given in Tables XI through XV. These bulk comparisons contain data from thick hazes and clouds and the clear atmospheres that could be represented by our Haze L model atmosphere. Thus all albedo ranges are included. One can note from the bulk measurements that the average albedo increases with wavelength.

Three special cases from this data sample are shown in Tables XVI through XVIII. The data in Table XVI and XVII are data from jungle areas, the first in Brazil, and the second from Cuba. During orbit 31, the data shown in Table XVI was taken with a solar zenith angle of 34°. The albedo for the four lower wavelengths are somewhat constant, and somewhat higher than the generally accepted values.

Table XI. Number of OSO-III Measurements Which Lie in Indicated Ground Albedo Ranges When Compared with the LITE-II Data for the Haze L Atmosphere: $\lambda=0.37\mu$

Incident Solar Angle (deg)	Ground Albedo Range									Total
	0.0-0.1	0.1-0.2	0.2-0.3	0.3-0.4	0.4-0.5	0.5-0.6	0.6-0.7	0.7-0.8	0.8-0.9	
0	2	4	2	2	1					11
10	5	18	25	22	21	11	6	3	3	114
20	59	199	25	11	11	9	3	1		417
30	96	337	177	59	28	15	4	5	2	723
40	85	272	333	103	20	36	13	8	3	933
50	85	338	221	135	86	49	38	40	14	1006
60	75	170	201	212	183	99	64	68	31	1103
70	15	44	84	120	151	164	140	99	66	883
80	3	17	12	19	24	25	45	35	43	222
85	1							1	1	3

Table XII. Number of OSO-III Measurements Which Lie in Indicated Ground Albedo Ranges When Compared with the LITE-II Data for the Haze L Atmosphere, λ=0.45μ

Incident Solar Angle (deg)	Ground Albedo Ranges									Total
	0.0-0.1	0.1-0.2	0.2-0.3	0.3-0.4	0.4-0.5	0.5-0.6	0.6-0.7	0.7-0.8	0.8-0.9	
0	1	3	6	2						12
10	13	23	36	28	9	5	4			118
20	145	180	49	15	7	6	2	3		407
30	195	325	126	28	9	9	2	2		696
40	306	408	127	48	24	22	3			938
50	130	395	195	81	61	36	22	31	11	962
60	203	313	195	179	79	71	49	15	5	1109
70	114	188	130	104	83	57	45	9		910
80	27	46	48	33	47	39	25	13	6	284
85	3	5	6	8	5	18	16	8	4	73

Table XIII. Number of OSO-III Measurements which Lie in Indicated Ground Albedo Ranges When Compared with the LITE-II Data for the Haze L Atmosphere: λ=0.54μ

Incident Solar Angle (deg)	Ground Albedo Range									Total
	0.0-0.1	0.1-0.2	0.2-0.3	0.3-0.4	0.4-0.5	0.5-0.6	0.6-0.7	0.7-0.8	0.8-0.9	
0	2	5	4	5						16
10	8	25	31	24	15	8	4	2		117
20	57	210	117	27	13	5		2	1	432
30	145	279	235	44	15	7	3	1		729
40	86	301	399	92	32	20	3	4		937
50	101	252	323	172	72	33	34	25	7	1019
60	127	240	318	196	104	73	43	18	9	1128
70	35	138	205	195	139	101	74	51	8	946
80	18	20	35	46	52	46	42	24	12	295
85	1	2		1	3	7	23	13	11	61

Table XIV. Number of OSO-III Measurements Which Lie in Indicated Ground Albedo Ranges When Compared with the LITE-II Data for the Haze L Atmosphere: $\lambda=0.67\mu$

Incident Solar Angle (deg)	Ground Albedo Range									Total
	0.0-0.1	0.1-0.2	0.2-0.3	0.3-0.4	0.4-0.5	0.5-0.6	0.6-0.7	0.7-0.8	0.8-0.9	
0	2	7	4	0	1					14
10	15	30	41	18	6	5	1			116
20	65	149	113	71	31	8	2	1		440
30	131	168	163	199	75	12	1			749
40	121	237	269	230	80	10	4	1		952
50	137	187	255	272	103	45	24	5		1028
60	126	217	311	261	127	53	24	10		1129
70	66	162	190	232	156	58	44	31	3	942
80	24	44	65	70	59	41	23	11	6	343
85	1	2	5	15	17	22	13	14	7	96

Table XV. Number of OSO-III Measurements Which Lie in Indicated Ground Albedo Ranges When Compared with the LITE-II Data for the Haze L Atmosphere: λ=0.78μ

Incident Solar Angle (deg)	Ground Albedo Range									Total
	0.0-0.1	0.1-0.2	0.2-0.3	0.3-0.4	0.4-0.5	0.5-0.6	0.6-0.7	0.7-0.8	0.8-0.9	
0	4	4	2	5	1					16
10	14	33	47	17	5					116
20	59	160	127	56	18					420
30	104	215	206	176	21	3				725
40	117	309	325	139	23	2				916
50	111	207	297	269	75	20				979
60	155	325	346	178	61	13	1			1079
70	147	216	253	179	65	13	1			874
80	65	101	59	36	13	8				282
85	20	16	21	4	2					63

Table XVI. Comparison of OSO-III and LITE-II Intensities for the Haze L Atmosphere: $\theta_o \simeq 34°$, $\cos\theta \simeq 0.78$, $\cos\phi \simeq -0.85$

Wavelength (μ)	Intensity (photons m^{-2}/source photon m^{-2})				
	LITE-II Data				OSO-III Data
	Albedo	Intnesity	Albedo	Intensity	
0.37	0.3	1.54-01	0.2	1.31-01	1.41-01
0.45	0.2	9.80-02	0.1	7.40-02	8.88-02
0.54	0.3	1.10-01	0.2	8.00-02	9.50-02
0.67	0.3	1.16-01	0.2	8.20-02	8.80-02
0.78	0.4	1.22-01	0.3	9.20-02	9.60-02

Table XVII. Comparison of OSO-III and LITE-II Intensities for the Haze L Atmosphere: $\theta_o \simeq 31.8°$, $\cos\theta \simeq 0.96$, $\cos\phi \simeq 0.06$

Wavelength (μ)	Intensity (photon m^{-2}/source photon m^{-2})				
	LITE-II Data				OSO-III Data
	Albedo	Intensity	Albedo	Intensity	
0.37	0.1	8.30-2	0.0	6.10-2	7.70-2
0.45	0.1	4.65-2	0.0	2.22-2	3.71-2
0.54	0.2	6.50-2	0.1	4.05-2	4.11-2
0.67	0.1	3.48-2	0.0	8.50-3	2.14-2
0.78	0.2	6.02-2	0.1	3.22-2	3.94-2

Table XVIII. Comparison of OSO-III and LITE-II Intensities for the Haze L Atmosphere: $\theta_o \simeq 30.5°$, $\cos\theta \simeq 0.99$, $\cos\phi \simeq -0.93$

Wavelength (μ)	Intensity (photons m^{-2}/source photon m^{-2})				
	LITE-II Data				OSO-III Data
	Albedo	Intensity	Albedo	Intensity	
0.37	0.2	9.13-2	0.1	7.13-2	8.90-2
0.45	0.2	7.33-2	0.1	4.95-2	5.84-2
0.54	0.3	1.00-1	0.2	7.40-2	8.20-2
0.67	0.4	1.45-1	0.3	1.14-1	1.30-1
0.78	0.4	1.17-1	0.3	8.98-2	9.46-2

This is attributed to the atmosphere having somewhat greater optical thickness than our model. The albedo for the larger wavelength (λ=0.78μ) increases as expected, and is of the correct order of magnitude. Because the albedo ranges from this sample of data indicated the optical thickness of the model was low, a second sample is presented from the same type of vegetation. The data in Table XVII yields albedo ranges that reproduce both the shape as a function of wavelength, and the generally accepted albedo values. The data in this sample shows the minimum albedo at λ=0.37μ with a slight increase to a maximum at the 0.54μ wavelength; a second decrease for λ=0.67μ and a second increase at λ=0.78μ.

Table XVIII shows a comparison of calculated data for the Haze L model atmosphere with OSO-III data taken over desert soil in Libya. The continental Haze L model is for a rather clear and dry atmosphere. The usually accepted albedo data for sand gives data ranges of 0.25 to 0.38 for λ=0.78μ, 0.18 to 0.30 for λ=0.67μ, 0.08 to 0.15 for λ=0.54μ, 0.05 to 0.12 for λ=0.45 and 0.05 to 0.11 for λ=0.37μ. When these values are compared with the LITE-II data and the OSO-III measurements in Table XVIII, the agreement is very good. With the exception of the data for λ=0.37μ which is approximately 10% high, each albedo range falls within the reported range. Again, with the change of surface type, the calculations method and the atmospheric model seen applicable to intensity calculations for near earth spacecraft.

VIII. SUMMARY AND CONCLUSION

A number of studies were conducted to determine the ability of the Monte Carlo calculation method to predict the reflected intensities at a near earth spacecraft. Five model atmospheres were formulated to give a library of data that would represent the various conditions observed by an orbiting satellite These values are in units of intensity per steradian and may be integrated over angle to yield the total radiant energy for a given wavelength at the spacecraft.

Monte Carlo calculations from the FLASH procedure for a spherical atmosphere were used in a study to determine the range of earth angles for which the calculational method used in RRA-89 can be expected to give accurate results. This study indicates that the range of angles is quite large. The RRA-89 results are accurate for earth angles varying from 0° to 90°, implying the total intensity at the satellite may be calculated accurately for almost all earth angles. For earth angles greater than 90°, the RRA-89 data will be approximatley 10% low.

A study was conducted to determine the effect of the surface albedo on the reflected intensitites. A comparison of the intensities calculated with a Lambert surface albedo was made with the intensities calculated for an isotropic scattering surface. The data for a Lambert type surface was approximately 30% above the data for an isotropic surface for polar reflection angles from 0° to 45°, in the 45° region the two calculations are approximately equal. Above 45°, the data for an

isotropic albedo for most incident angles are larger than the data for the Lambert surface, in some cases this difference is 40%. We feel that the data for the Lambert surface is more realistic.

The angular distribution of reflected radiation from our cloud models was compared with the average angular distribution observed from the TIROS satellite. Exact comparisonsbetween the TIROS data and our calculated data can not be made because of the different wavelengths and incident solar angles. However, the general shape of the angular distribution calculated in this study and the published angular distributions are in good agreement.

When the calculated intensities for the clear maritime and continental atmospheric models were compared with the OSO-III data, general good agreement was found. The Monte Carlo calculations give both the magnitude and the angular variation of the reflected intensity measured by the OSO-III spacecraft with the exception of the measurements made with a large solar incident angle. This difference, observed here for measurements over water, is interpreted as due to Fresnel type reflection.

The OSO-III measurements of reflected radiation from clouds were compared with the Monte Carlo calculations for a model atmosphere containing a cloud with an optical thickness of approximately 80. These comparisons were generally good. There was a tendency of the calculated data to slightly over-predict the observed intensity.

This slight over-prediction is believed to be due to the single scattering albedo used in the model.

The good agreement between the calculated and experimental values is sufficiently close to warrant the conclusion that most problems involving the reflected radiation from a planetary surface covered by an atmosphere may be solved using these techniques. The accuracy of the estimated intensity is limited only by the ability to define a model atmosphere and surface. In most cases an average model yields reliable results, and the effort to gain a few percent more accurate results with the more realistic models may not be justified.

1. Collins, Dave G and Wells, Michael B., Monte Carlo Codes for Study of Light Transport in the Atmosphere, RRA-T54, Volumes I and II, Radiation Research Associates, Inc. (1965)

2. Wells, Michael B., Collins, Dave G., and Cunningham, Kelly, Light Transport in the Atmosphere, RRA-T63, Volumes I, II, II, Radiation Research Associates, Inc. (1966).

3. Wells, Michael B., and Marshall, J. D., Monochromatic Light Intensities above the Atmosphere Resulting from Atmospheric Scattering and Terrestrial Reflection, RRA-T85, Radiation Research Associates, Inc (1968).

4. D. Deirmenjian, Electromagnetic Scattering on Spherical Poly-Dispersion, Elsener Publishing Company, Inc. (1969).

5. Elterman L., Atmospheric Attenuation Model, 1964, in the Ultra-Violet, Visible, and Infared Regions for Altitudes to 50 km., AFCRL-64-740, (1964).

6. Carrier, L. W., Cato, G. A., and von Essen, K. J., Applied Optics, Vol. 6. No. 7. (1967).

7. Wells, M. B. and Collins, D. C., FLASH, A Monte Carlo Procedure for Use in Calculating Light Scattering in A Spherical Shell Atmosphere, RRA-T704, Radiation Research Associates, Inc. (1970).

8. Ruff, I., Koffler, R., Fritz, S., Winston, J. S., and Rao, P. K., Journal of Atmospheric Sciences, Vol, 25, No. 2. 323 (1968).

9. Valley, Shea L, editor, Handbook of Geophysics and Space Environments, McGraw Hill Book Co. (1965).

10. Griffin, R. N., and Beck, C. W., "Description of Ames Research Center Earth Albedo Experiment on OSO-III Spacecraft" NASA publication, Ames Research Center, Moffett Field, California.

11. Griggs, M. J., Applied Meteor. 7, 1012. (1968).

12. Danielson, R. E., Moore, D. R , and van de Hulst, Journal of the Atmospheric Sciences, 26, 1078, (1969).

13. Brennan, B., "Bidirectional Reflectance Measurements from an Aircraft Over Natural Earth Surfaces" (NASA-TM-X-63564), May 1969.